JACS
JOURNAL OF THE AMERICAN CHEMICAL SOCIETY
Article
pubs.acs.org/JACS

Manifestation of Polar Reaction Pathways of 2,3-Dichloro-5,6-dicyano-*p*-benzoquinone

Xingwei Guo and Herbert Mayr*

Department Chemie, Ludwig-Maximilians-Universität München, Butenandtstraße 5-13 (Haus F), 81377 München, Germany

Supporting Information

ABSTRACT: Reactions of 2,3-dichloro-5,6-dicyano-*p*-benzoquinone (DDQ) with silyl enol ethers, silyl ketene acetals, allylsilanes, enamino esters, and diazomethanes have been studied in CH_3CN and CH_2Cl_2 solutions. The second-order rate constants for C attack at DDQ (log k_C) correlate linearly with the nucleophile-specific parameters N and s_N and are 2−5 orders of magnitude larger than expected for SET processes, which strongly supports the polar mechanism for C−C bond formation. The second-order rate constants for O attack agree well with the calculated rate constants for rate-determining single electron transfer (SET). As a radical clock experiment ruled out outer sphere electron transfer, an inner sphere electron transfer mechanism is suggested for O attack.

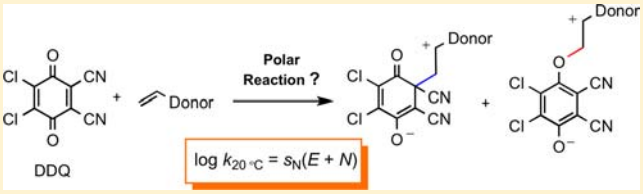

INTRODUCTION

2,3-Dichloro-5,6-dicyano-*p*-benzoquinone (DDQ), first synthesized by Thiele and Günther in 1906,[1] has a high redox potential (0.54 V vs SCE in acetonitrile)[2] and is one of the most important oxidizing reagents in organic chemistry. It usually reacts as a one-electron acceptor to give a radical anion in the first step and has been used for the oxidation of steroid ketones, hydroaromatic compounds, alcohols, phenols, and heterocycles.[3] Recently, DDQ was used as an oxidant for several oxidative coupling reactions.[4]

Triggered by the observation of DDQ-substrate adducts during the oxidation of 4-aza-3-ketosteroids by DDQ,[5] Bhattacharya and co-workers investigated the reactions of cyclic silyl enol ethers with DDQ and found the formation of adducts **3a-C** and **3a-O** (Scheme 1).[6]

The dramatic solvent and temperature effects on the product ratios were considered to be indicative of the operation of two distinctly different pathways for the formation of **3a-C** and **3a-O**. Though both products were suggested to be formed via a radical ion pair, the possibility of a nucleophilic attack of the silyl enol ether on DDQ to form the carbon−carbon adduct **3a-C** was explicitly mentioned as an alternative.[6] We now report kinetic investigations of the reactions of DDQ with π-nucleophiles, which clearly show that polar mechanisms are rather the rule than the exception for these reactions.

In recent years, we have developed a linear free energy relationship based model for polar organic reactions,[7] which uses eq 1 to predict rates and selectivities for these reactions:

$$\log k(20°C) = s_N(E + N) \quad (1)$$

In eq 1 the second-order rate constant (log k) is calculated by two nucleophile-specific parameters s_N and N and one electrophile-specific parameter E. A comprehensive nucleophilicity scale covering more than 30 orders of magnitude[8] has been created by using a series of benzhydrylium ions and structurally related quinone methides as reference electrophiles.[9] We have now used the linear free energy relationship (1) to elucidate the mechanisms of the reactions of DDQ with π-systems (Table 1).

RESULTS

Product Studies in Acetonitrile. In line with earlier investigations,[6] the cyclic silyl enol ethers **2a−c** were found to give predominantly **4(a-c)-C**, the products of C attack in acetonitrile, and only a trace (~4%) of **4b-O**, the product of O attack, was detected by ^{1}H NMR spectroscopy (Scheme 2). Compounds **4(a-c)-C** were isolated as mixtures of diastereomers after column chromatography. The major diastereomers of **4(a,c)-C** were obtained and characterized as pure compounds by recrystallization from a mixture of dichloromethane and pentane. Additionally, the major diastereoisomer of **4a-C** was characterized by X-ray crystallography (Figure 1).

The reactions of the terminal silyl enol ethers **2d** and **2e** and silyl ketene acetals **2f** and **2g** with DDQ yielded the products of C attack (**4(d-g)-C**) quantitatively (Scheme 3), which were purified by column chromatography.

While the isobutyraldehyde-derived silyl enol ether **2h** reacted via O attack to give 68% of **3h-O** and 32% of the dehydrogenated product **5h** (Scheme 4), according to ^{1}H NMR analysis of the crude reaction product, the structurally analogous silyl ketene acetal **2i** reacted with DDQ preferentially at carbon to give 94% of **3i-C** and 6% of **3i-O**. At elongated reaction times **3i-C** slowly transformed into a mixture of **3i-O** and **5i** (Scheme 4). The parallel increase of **3i-O** and **5i** (Figure 2) shows that both products are formed in parallel reactions

Received: June 12, 2013
Published: July 24, 2013

   dx.doi.org/10.1021/ja405890d | *J. Am. Chem. Soc.* 2013, 135, 12377−12387

Scheme 1. Reaction of DDQ (1) with the Silyl Enol Ether 2a as Suggested by Bhattacharya et al.[6]

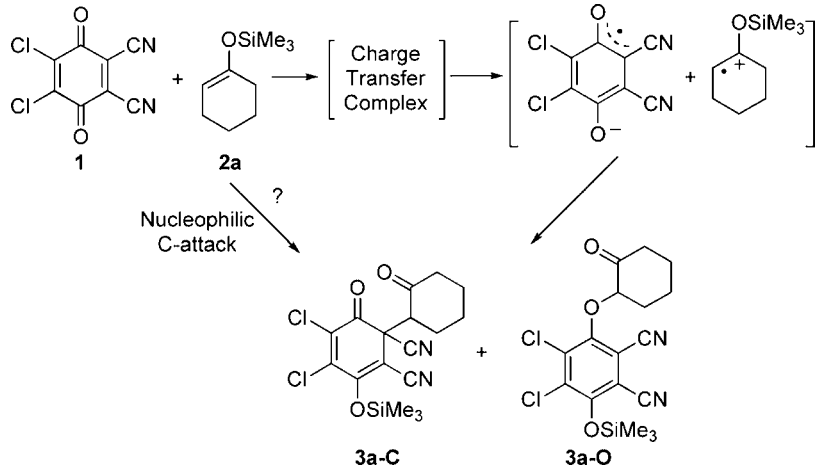

Table 1. Nucleophiles 2a–o and Their Reactivity Parameters N and s_N in CH_2Cl_2

Nucleophile			N (s_N)[a]
	**2a**	$n = 2$	5.21 (1.00)
	2b	$n = 1$	6.57 (0.93)
	2c	$n = 3$	6.62 (1.00)
	**2d**	R = Ph	6.22 (0.96)
	2e	R = Me	5.41 (0.91)
	2f	R = OPh	8.23 (0.81)
	2g	R = OBu	10.21 (0.82)
	**2h**	R = H	3.94 (1.00)
	2i	R = OMe	9.00 (0.98)
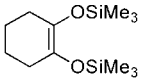	**2j**		4.61 (1.19)[b]
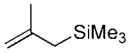	**2k**		4.41 (0.96)
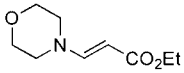	**2l**		8.52 (0.80)
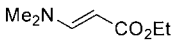	**2m**		9.43 (0.80)
	**2n**	R = Ph	9.35 (0.83)
	2o	R = COOEt	4.91 (0.95)

[a]From ref 8. [b]This work.

from **3i-C** and excludes the generation of **5i** by elimination from **3i-O**. In view of the slow conversion of **3i-C** into **3i-O** (after 10 min, only 7% of **3i-O** are present), the observation of a small amount of **3i-O** even after 1 min indicates that 6% of **3i-O** is directly formed from DDQ and **2i** (kinetic product control). The desilylated products **4h-O** and **4i-O** were

Scheme 2. Reactions of DDQ with Cyclic Silyl Enol Ethers 2a–c

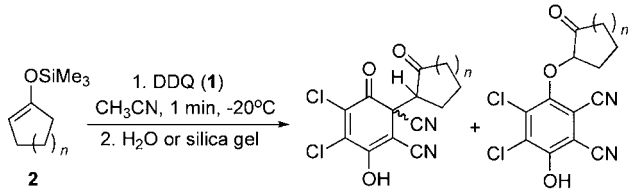

2a ($n = 2$)	**4a-C**	(83%, *dr* 6 : 1)[a]	**4a-O** (< 4%)[b]
2b ($n = 1$)	**4b-C**	(87%, *dr* 2 : 1)[a]	**4b-O** (4%)
2c ($n = 3$)	**4c-C**	(83%, *dr* > 30 : 1)[a]	**4c-O** (< 4%)[b]

[a]Isolated yield. [b]Not observed by ^{1}H NMR in the crude material.

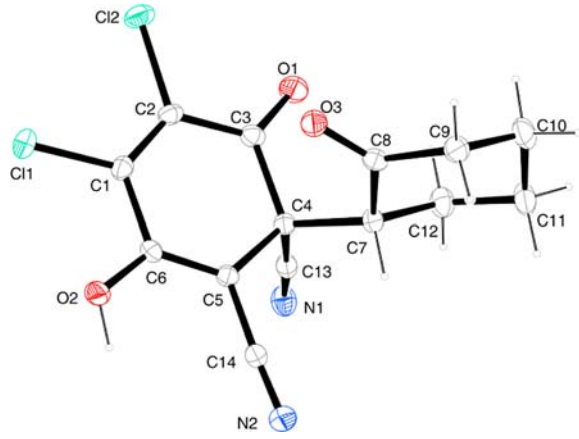

Figure 1. Crystal structure of **4a-C** (major diastereomer, thermal ellipsoids are drawn at the 50% probability level).

obtained by column chromatography on silica gel in 45 and 63% yield, respectively (see the Supporting Information).

The rearrangement of **3i-C** to **3i-O** can be assumed to proceed via a radical pathway, as shown in Scheme 5. When (2,2,6,6-tetramethylpiperidin-1-yl)oxyl (TEMPO) was added to crude **3i-C**, which was formed from **1** and **2i** in CH_3CN within 1 min (Scheme 4), a 45: 55 mixture of **3i-O** and **6** was formed within 72 h at room temperature (^{1}H NMR). Methyl methylacrylate **5i** probably was lost during evaporation of the solvent. Column chromatography of the mixture provided pure **6** in 49% yield, which was fully characterized.

dx.doi.org/10.1021/ja405890d | J. Am. Chem. Soc. 2013, 135, 12377–12387

Scheme 3. Reactions of DDQ with Terminal Silyl Enol Ethers and Ketene Acetals

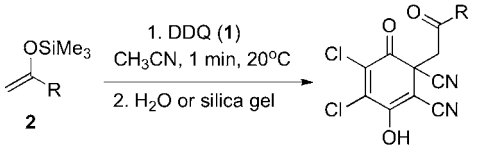

2d (R = Ph) **4d-C** (97%)
2e (R = Me) **4e-C** (97%)
2f (R = OPh) **4f-C** (83%)
2g (R = O*n*Bu) **4g-C** (79%)

Scheme 4. Relative Yields (^{1}H NMR) of the Reactions of DDQ with 2h and 2i in CD_3CN

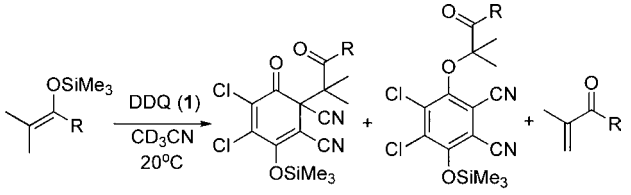

2h (R = H)	1 min	**3h-C**	*n.d.*[a]	**3h-O**	68 %	**5h**	32 %
	1 h		*n.d.*[a]		68 %		32 %
2i (R = OMe)	1 min	**3i-C**	94 %	**3i-O**	6 %	**5i**	*n.d.*[a]
	10 min		93 %		7 %		*n.d.*[a]
	1 h		82 %		16 %		2 %
	22 h		28 %		57 %		15 %
	48 h		8 %		70 %		22 %
	72 h		4 %		72 %		24 %

[a] *n.d.* = not detected.

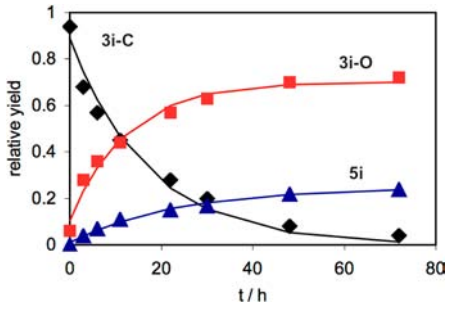

Figure 2. Time resolved relative ^{1}H NMR yields of **3i-C**, **3i-O**, and **5i** during the reaction of DDQ with **2i** (in CD_3CN, at 20 °C).

The reaction of 1,2-disiloxycyclohexene **2j** with DDQ gave exclusively the product of O attack (Scheme 6). The partially desilylated product **4j-O** crystallized from CH_2Cl_2/pentane solution and was analyzed by X-ray crystallography (Figure 3).

The reaction of allylsilane **2k** with DDQ initially gave **3k-C**, the product of C attack, that slowly rearranged into the allyl phenyl ether **3k-O** (Scheme 7). After hydrolysis, the desilylated derivative **4k-O** was obtained by crystallization in 81% yield (see the Supporting Information).

Previous investigations have shown that DDQ reacts with the secondary enaminoester **7** to give the spirane **9** (Scheme 8), indicating that **7** attacks at C-2 of DDQ.[10] In this work, we observed the exclusive formation of **3l-O** from **1** and the tertiary enaminoesters **2l** or **2m** after aqueous workup, which can be explained through O attack and formation of **10** as illustrated in Scheme 8. Proton migration, cyclization, hydrolysis, and decarbonylation eventually yield benzofuran

Scheme 5. Trapping of the Intermediate of the Rearrangement of 3i-C to 3i-O

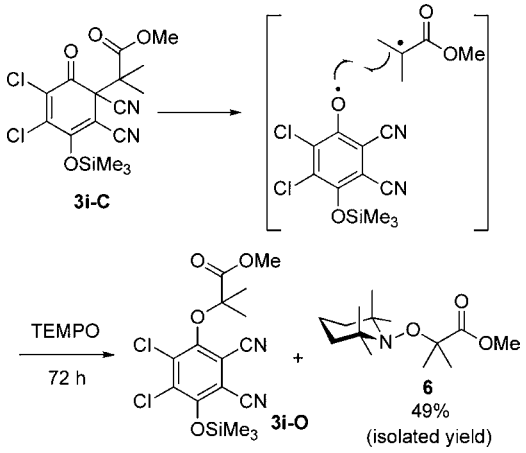

Scheme 6. Reaction of DDQ with 2j

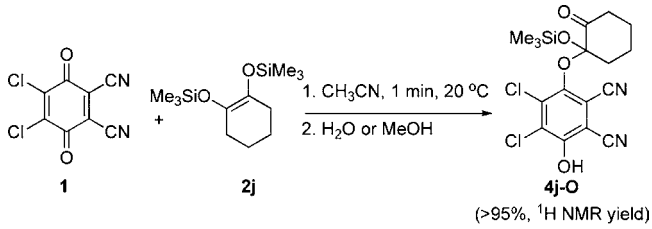

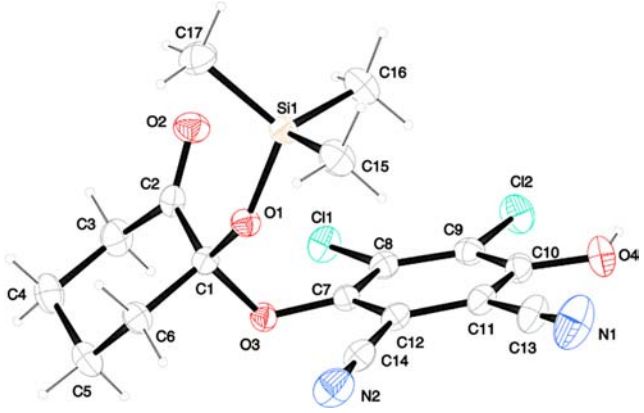

Figure 3. Crystal structure of **4j-O** (thermal ellipsoids are drawn at the 50% probability level).

3l-O as the final product. Possibly, **2l** and **2m** initially also attack **1** at the carbon, to give a zwitterion analogous to **8**, which cannot cyclize to a spirane because of the absence of an NH proton. Therefore, it may revert to reactants and subsequently react via O attack to give **3l-O** as the final product.

While the reaction of phenyldiazomethane with DDQ gave 92% of the bicyclic diketone **3n-C** (diastereomer ratio: ca. 55/45), no reaction between ethyl diazoacetate and DDQ was observed at room temperature within 1 h (Scheme 9).

Solvent Effect. Scheme 10 shows that the **4a-O**/**4a-C** ratio generated by the reaction of DDQ with **2a** depends strongly on the concentration of the reactants and on the solvent. According to entries 1 and 2, the **4a-O**/**4a-C** ratio increases from 40/60 to 92/8 when reducing the concentration of **2a** from 0.1 to 0.02 mol L^{-1} in CH_2Cl_2. In the dilute solution (0.02

dx.doi.org/10.1021/ja405890d | J. Am. Chem. Soc. 2013, 135, 12377−12387

Scheme 7. Reaction of DDQ with 2k

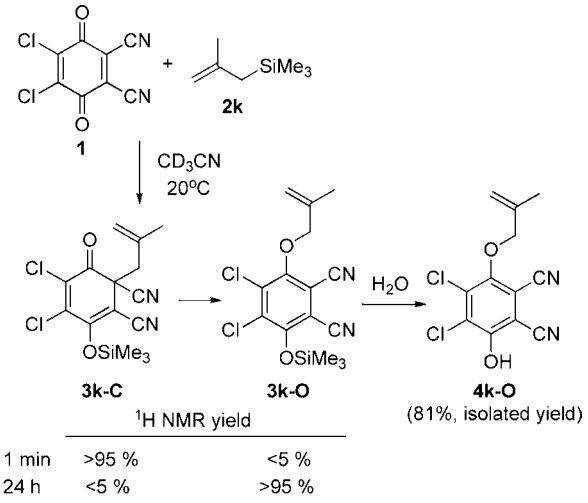

mol L^{-1}), the **4a-O**/**4a-C** ratio decreases dramatically from 92/8 to 7/93 when the solvent is changed from CH_2Cl_2 to CH_2Cl_2/MeOH, and CH_3CN (entries 2−7, Scheme 10). In acetonitrile solution, the product ratio is neither affected by the concentration of **2a** nor by the presence of methanol (entries 7−10, Scheme 10). As **3a-C** does not rearrange into the thermodynamically more stable isomer **3a-O** when dissolved in CD_2Cl_2 (Scheme 11), we can rule out isomerization at the product stage.

When the *tert*-butyldimethylsilyl substituted enol ether **2a′** was used, more product of O attack was observed than in the corresponding reactions with the trimethylsilyl substituted compound **2a** in both CH_2Cl_2 and CH_3CN (entries 2/11 and 7/12, Scheme 10). In the reactions of DDQ with **2a′**, the **4a-O**/**4a-C** ratio decreases when methanol is added to acetonitrile

Scheme 9. Reactions of DDQ with Diazoalkanes

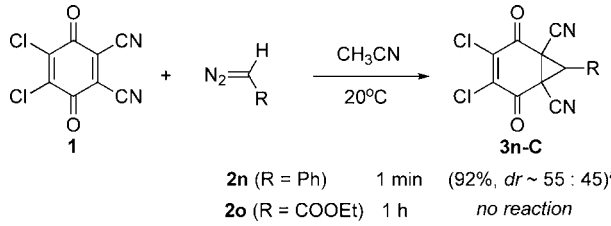

[a]Yield and *dr* (^{1}H NMR) correspond to the crude product; only the major isomer was isolated and characterized.

and reaches a constant value of 7/93 for >10% of MeOH (entries 13−17, Scheme 10).

A rationalization for these observations is given in Scheme 12. Attack of **2a** at a carbon of DDQ to give **11** is faster than O attack to give **12**. As silyl shifts to convert **11** into **3a-C** and **12** into **3a-O** cannot occur intramolecularly, silyl-carriers are needed. Such a carrier may be the solvent when the reacton is carried out in acetonitrile solution (→ *N*-trimethylsilyl-nitrilium ions). As the product ratio [**4a-O**]/[**4a-C**] obtained from **2a** is not affected by addition of the stronger nucleophile methanol in acetonitrile, we conclude that **11** and **12** are formed irreversibly in acetonitrile solution due to the fast subsequent silyl shift, and that the product ratio [**4a-O**]/[**4a-C**] = 7/93 corresponds to k_O/k_C. The independence of the observed rate constants k_{obs} (for measurements see below) of methanol additives (Figure 4) and NBu_4OTs additives (Tables S1 and S11, see the Supporting Information) are in line with this interpretation.

Because of its lower nucleophilicity, dichloromethane cannot act as a silyl-carrier, and the conversions **11** → **3a-C** and **12** → **3a-O** can only occur in the presence of other nucleophiles, e.g., methanol, or when bimolecular reactions of two molecules of **11** or **12** lead to the formation of **3a-C** and **3a-O**. In the

Scheme 8. Reactions of DDQ with Enamino Esters

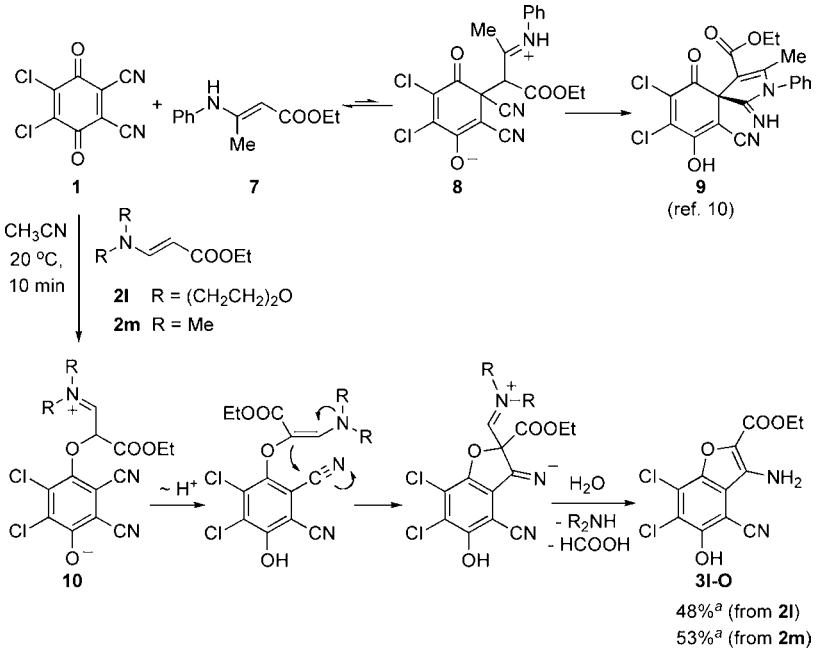

[a]Yield isolated after crystallization from AcOH/CH_3CN

dx.doi.org/10.1021/ja405890d | J. Am. Chem. Soc. 2013, 135, 12377−12387

Scheme 10. Solvent Effect on the Reaction of DDQ with 2a and 2a′

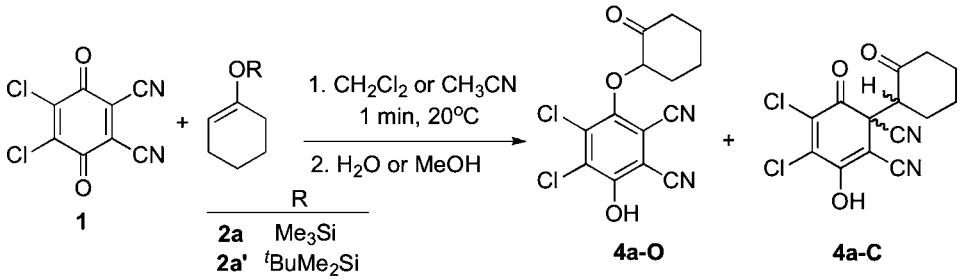

entry	nucleophile	solvent	[**2a** or **2a'**][a]/ mol L^{-1}	relative yield[b]/%	
				4a-O	**4a-C**
1	**2a**	CH_2Cl_2	0.1	40	60 (58:42)
2		CH_2Cl_2	0.02	92	8 (50:50)
3		CH_2Cl_2 (1% MeOH)	0.02	39	61 (74:26)
4		CH_2Cl_2 (4% MeOH)	0.02	22	78 (41:59)
5		CH_2Cl_2 (10% MeOH)	0.02	14	86 (36:64)
6		CH_2Cl_2 (20% MeOH)	0.02	9	91 (29:71)
7		CH_3CN	0.02	7	93 (25:75)
8		CH_3CN	0.1	7	93 (25:75)
9		CH_3CN (1% MeOH)	0.1	7	93 (25:75)
10		CH_3CN (10% MeOH)	0.1	6	94 (22:78)
11	**2a'**	CH_2Cl_2	0.02	>95	<4
12		CH_3CN	0.02	30	70 (50:50)
13		CH_3CN	0.1	33	67 (51:49)
14		CH_3CN (1% MeOH)	0.1	25	75 (51:49)
15		CH_3CN (5% MeOH)	0.1	11	89 (45:55)
16		CH_3CN (10% MeOH)	0.1	7	93 (41:59)
17		CH_3CN (20% MeOH)	0.1	7	93 (34:66)

[a]In all cases, 10 equiv of **2a** or **2a′** were used, that is, [**2a** or **2a′**]/[**1**] = 10. [b]Quantitative product formation, ratios of diastereoisomers were determined by ^{1}H NMR of the crude product mixture and are given in parentheses (see the Supporting Information for details).

Scheme 11. Examination of Product Stability of 3a-C in CD_2Cl_2

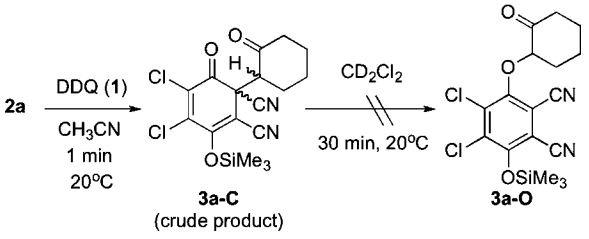

absence of methanol or in highly dilute solutions in dichloromethane, silyl transfers will be slow, and the formation of **11** that is thermodynamically less stable than **12** will be reversible. As a consequence, in highly dilute dichloromethane solutions (where also the concentrations of **11** and **12** will be small), the ratio [**3a-O**]/[**3a-C**] will be large because of the reversible formation of **11**. Already small amounts of methanol are sufficient to accelerate the silyl transfer, which results in an increase of the observed rate constant (factor of 2 in a 0.05 mol L^{-1} solution, Figure 4) as well as the yield of **3a-C**.

The observations with the *t*$BuMe_2Si$ substituted enol ether **2a′** are in line with these interpretations. As the transfer of the sterically more shielded *t*$BuMe_2Si$ group is slower than that of the Me_3Si group, in dilute dichloromethane solution, C attack at DDQ becomes completely reversible, and **4a-O** is the only product (entry 11, Scheme 10). In pure acetonitrile, C attack (which is irreversible with **2a**, see above) becomes partially reversible in the reaction with **2a′**, and addition of the more nucleophilic methanol now leads to a decrease of the ratio [**4a-O**]/[**4a-C**] (entries 13−17, Scheme 10).

Charge Transfer (CT) Complexes. The formation of CT complexes between electron-deficient and electron-rich π-systems is well-known.[11] As the association constants between the nucleophiles **2** and DDQ (**1**) are small, at room temperature the corresponding CT complexes could only be observed in few cases as short-lived intermediates when high concentrations of the reactants were employed. Since lowering of the temperature increases the association constants and retards the reactions of **1** with **2**, we have been able to observe several CT complexes, however, when mixing the nucleophiles **2** with DDQ in CH_2Cl_2 at −80 °C (Scheme 13). The new absorption bands observed under these conditions can be assigned to charge transfer complexes, because neither DDQ nor the nucleophiles **2** examined absorb beyond 450 nm.

Though the CT complexes are likely to correspond to the encounter complexes preceding the formation of the reaction products from **1** and **2**, the kinetic data do not allow us to differentiate whether the CT complexes are intermediates on

dx.doi.org/10.1021/ja405890d | J. Am. Chem. Soc. 2013, 135, 12377−12387

Scheme 12. Possible Mechanism of the Reaction of DDQ with 2a

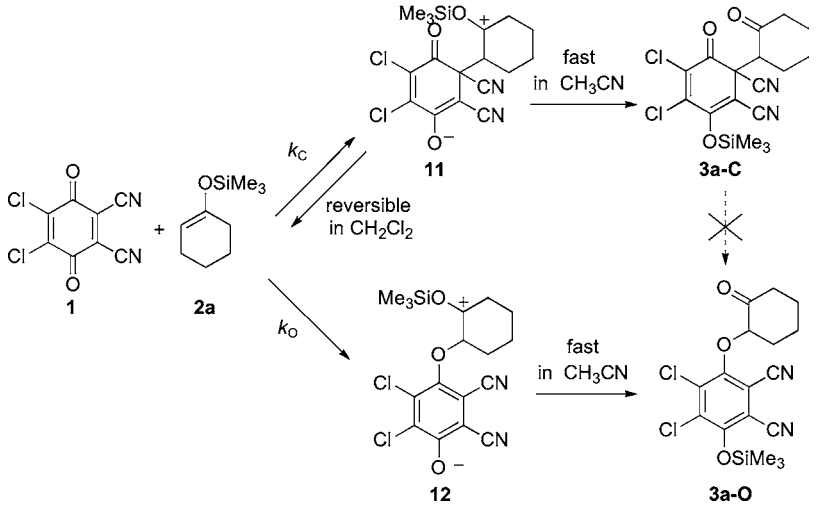

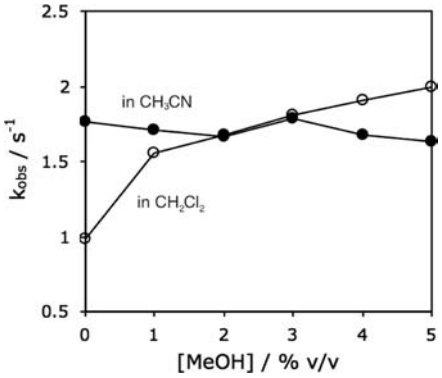

Figure 4. Effect of methanol on the rate of the reaction of DDQ (5.0×10^{-3} mol L^{-1}) with **2a** (5.0×10^{-2} mol L^{-1}) in CH_2Cl_2 and in CH_3CN (monitoring the CT complex at 570 nm).

Scheme 13. Characteristic Absorption Bands of the CT Complexes of Nucleophiles 2 with DDQ in CH_2Cl_2 at −80 °C

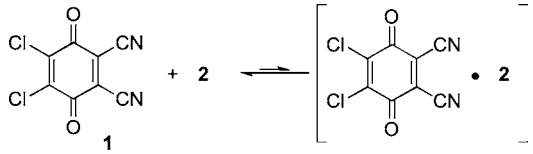

2	$\lambda_{max,CT}$ / nm
2a	589
2b	578
2c	574
2d	592
2h	569
2l	719
2m	709

the way to the products or correspond to dead ends of a nonproductive side channel (Curtin-Hammett principle[12]).

Kinetic Studies. All kinetic investigations of the reactions of DDQ with the nucleophiles **2** were performed in acetonitrile or dichloromethane solution at 20 °C. The reactions were monitored by UV−vis spectroscopy at or close to the absorption maxima of DDQ (278 nm, Figure 5). For some nucleophiles (**2d**, **2l**, and **2m**), the formation of the products

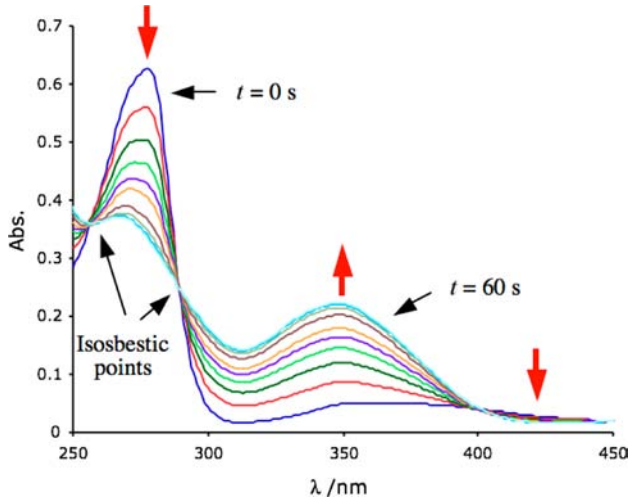

Figure 5. Time-dependent UV−vis absorbance during the reaction of DDQ (1.0×10^{-4} mol L^{-1}) with **2e** (3.9×10^{-3} mol L^{-1}) in CH_3CN at 20 °C.

was monitored (at 350 nm) because of the intensive absorbance of nucleophiles at lower wavelength (<300 nm). Pseudo first-order rate constants k_{obs} were obtained by least-squares fitting of the absorbances to the monoexponential function $A_t = A_0 e^{-k_{obs}t} + C$ or $A_t = A_0 (1 - e^{-k_{obs}t}) + C$. Second-order rate constants k_2 were derived from the linear correlation of k_{obs} (s^{-1}) with the concentrations of the nucleophiles (Figure 6).

In line with the fast reversible formation of the CT complexes, identical rate constants for the reaction of DDQ with **2a** were derived by following the decay of the absorption band of the CT complex (589 nm) and the absorption band of DDQ (286 nm) as well as the increase of the absorption of the product (350 nm) in CH_2Cl_2 at −60 °C (Figure 7).

The observation of second-order kinetics for the reactions of DDQ with nucleophiles **2** in CH_2Cl_2 is surprising in view of the discussion of Schemes 10 and 12. Possibly, the perfect linearity of the k_{obs} vs [**2**] correlations (Tables S15−S21) indicates that

dx.doi.org/10.1021/ja405890d | J. Am. Chem. Soc. 2013, 135, 12377−12387

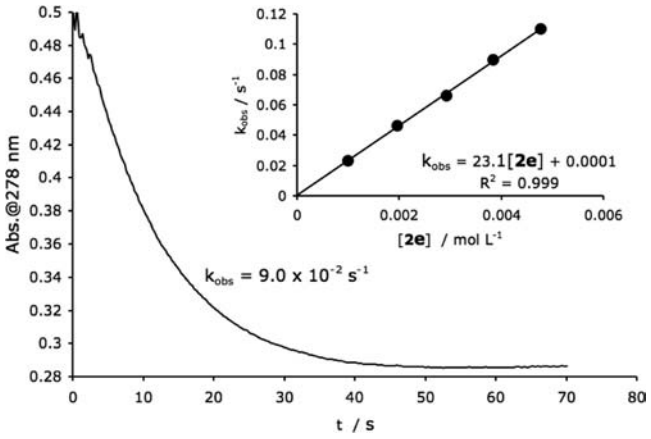

Figure 6. UV−vis spectroscopic monitoring of the reaction of DDQ (1.0×10^{-4} mol L^{-1}) with **2e** (3.9×10^{-3} mol L^{-1}) at 278 nm in CH_3CN at 20 °C. Insert: Determination of the second-order rate constant k_2 = 23 L mol^{-1} s^{-1} from the dependence of the first-order rate constant k_{obs} on the concentration of **2e**.

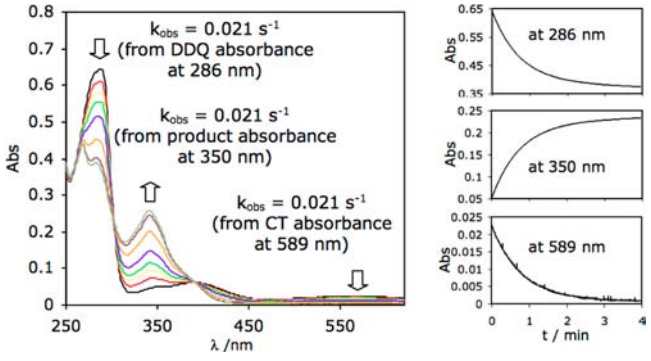

Figure 7. UV−vis spectra of a mixture of DDQ (1.0×10^{-4} mol L^{-1}) and **2a** (4.0×10^{-3} mol L^{-1}) in CH_2Cl_2 at −60 °C and the time dependent UV−vis absorbance at 286, 350, and 589 nm.

also **2a-f,k** may act as silyl carriers under the conditions of the kinetic experiments.

Table 2 shows that the ratios of the second-order rate constants for the reactions of DDQ with nucleophiles **2** in CH_2Cl_2 and CH_3CN solutions, $k_2^{CH_2Cl_2}/k_2^{MeCN}$, vary from 0.44 to 3.1 indicating that the kinetics are only slightly affected by solvent polarity.

Ab Initio Calculation of Adiabatic Ionization Potentials. In order to elucidate the feasibility of single electron transfer (SET) processes, we have determined the ionization potentials of the π-nucleophiles **2(a-q)** by quantum chemical calculations using the Gaussian 09 program package.[13] Adiabatic ionization potentials were calculated at the G3(MP2) level of theory, which is a high-level composite ab initio molecular orbital theory method as the sum of the CCSD(T) calculations with a double-ζ basis set and basis set corrections carried out at the MP2 level of theory to approximate CCSD(T) calculations with a large triple-ζ basis. G3(MP2) has been shown to reproduce a large test set of gas-phase experimental data within chemical accuracy.[14] The adiabatic ionization potentials listed in Table 3 have been calculated as the difference of the enthalpies of the radical cations and those of the neutral molecules in the gas phase.

Table 3. Calculated Adiabatic Ionization Potentials [G3(MP2)] of Nucleophiles 2 and the Corresponding Electrochemical Oxidation Potentials

nucleophile	IP_a/eV	E_{ox} (vs SCE)/V
2a	7.77	1.30[a]
2b	7.83	1.21[b]
2c	7.71	1.15[b]
2d	8.10	1.32[a]
2e	8.24	1.43[b]
2f	7.89	1.24[b]
2g	7.65	1.12[b]
2h	7.77	1.18[b]
2i	7.22	0.90[a]
2j	7.05	0.80[b]
2k	8.26	1.44[b]
2l	7.71	1.15[b]
2m	7.70	1.14[b]
2n	7.87	1.23[b]
2p[c]	8.48	1.50[a]
2q[c]	7.18	0.83[a]

[a]In CH_3CN from ref 15. [b]Calculated by substitution of calculated ionization potentials into eq 2. [c]See Figure 8 for the structures of these compounds.

Figure 8 shows that the calculated ionization potentials correlate with the experimental oxidation potentials[15] of **2a**, **2d**,

Table 2. Second-Order Rate Constants *k* for the Reaction of DDQ with Nucleophiles (2a−n) at 20 °C

nucleophile	$k_2^{CH_2Cl_2}$/L mol^{-1} s^{-1}	k_2^{MeCN}/L mol^{-1} s^{-1}	$k_2^{CH_2Cl_2}/k_2^{MeCN}$	k_O/L mol^{-1} s^{-1} (in CH_3CN)	k_C/L mol^{-1} s^{-1} (in CH_3CN)
2a	1.9×10^1	2.5×10^1	0.76	1.9	2.3×10^1
2b	3.4×10^2	5.5×10^2	0.62		5.5×10^2
2c	9.6×10^2	7.1×10^2	1.4		7.1×10^2
2d	2.0×10^2	4.5×10^2	0.44		4.5×10^2
2e	4.5×10^1	2.3×10^1	2.0		2.3×10^1
2f	1.1×10^4	3.5×10^3	3.1		3.5×10^3
2g		8.5×10^5			8.5×10^5
2h		1.8×10^{-1}		1.8×10^{-1}	
2i		1.1×10^7		6.6×10^5	1.0×10^7
2j		7.0×10^4		7.0×10^4	
2k	3.9×10^{-1}	3.9×10^{-1}	1.0		3.9×10^{-1}
2l		6.8		6.8	
2m		2.3×10^1		2.3×10^1	
2n		8.6×10^3			8.6×10^3

dx.doi.org/10.1021/ja405890d | J. Am. Chem. Soc. 2013, 135, 12377−12387

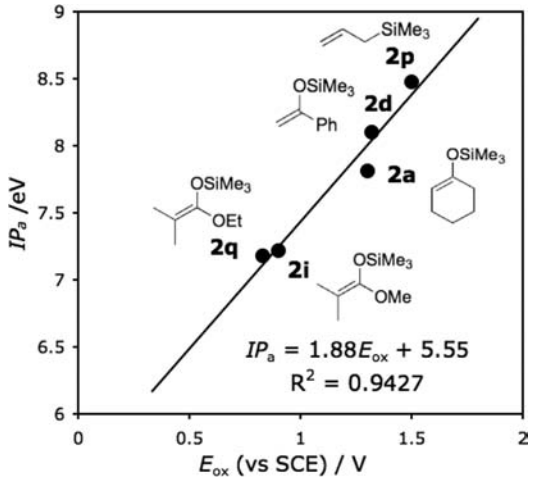

Figure 8. Correlation between calculated adiabatic ionization potentials IP_a and experimental oxidation potentials E_{ox} (vs SCE in CH_3CN).

2i, **2p**, and **2q** as expressed by eq 2, which is similar to the correlation previously reported for aromatic compounds ($IP_a = 1.5E_{ox} + 5.8$).[16] Using correlation (2) we have calculated experimentally not available oxidation potentials from their adiabatic ionization potentials (Table 3).

$$IP_a = 1.88E_{ox} + 5.55 \quad (2)$$

DISCUSSION

Correlation Analysis. In order to examine the validity of eq 1 for the reactions of DDQ (C attack) with π-nucleophiles, a plot of $(\log k_C)/s_N$ against the nucleophilicity parameters N of nucleophiles is presented in Figure 9. A fair linear correlation ($R^2 = 0.91$) was obtained.

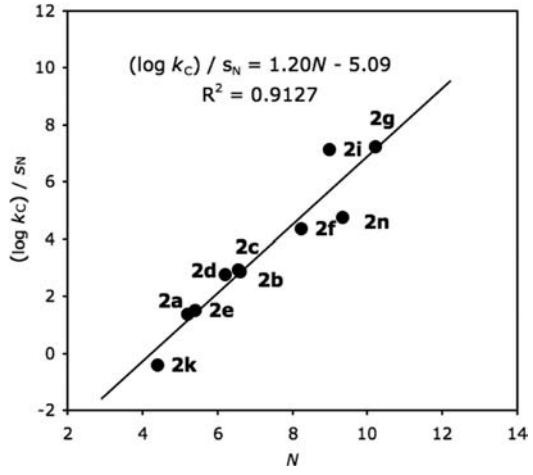

Figure 9. Plot of $(\log k_C)/s_N$ vs N for the reactions of DDQ (C attack) with π-nucleophiles in CH_3CN at 20 °C.

According to eq 1, the electrophilicity parameter of DDQ (reactivity at C-2) was determined as $E = -3.66$ by least-squares minimization of $\Delta^2 = \Sigma(\log k_C - s_N(N + E))^2$ using the second-order rate constants k_C given in Table 2 and the N and s_N parameters of the nucleophiles **2a**-**n** from Table 1.

In previous work we have shown that the electrophilicity parameters of benzhydrylium ions and structurally related quinone methides correlate linearly with their reduction potentials (Figure 10).[17] When the data for DDQ are added

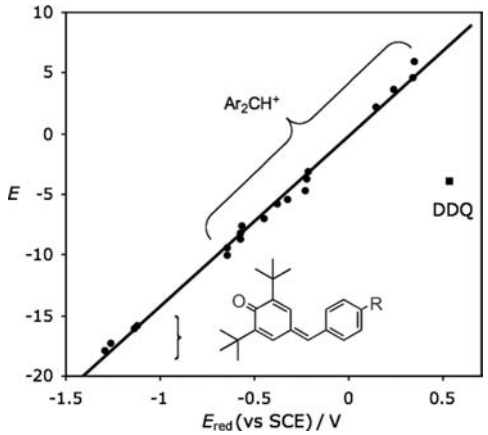

Figure 10. Correlation between the electrophilicity parameters E and the reduction potentials E_{red} of reference electrophiles[17] and DDQ.

to this correlation, one can see that DDQ reacts much more slowly with π-nucleophiles than expected from its reduction potential. The position of DDQ in Figure 10 implies that the transition states of the reactions of DDQ with π_{CC} systems profit much less from the formation of the new CC bond (product stabilizing factor) than the corresponding reactions of benzhydrylium ions and quinone methides. Yu and co-workers have demonstrated recently that a relationship between electrophilicities E and LUMO energies holds only within species that share similar substitution patterns.[18] Thus, arylidene Meldrum's acids and arylidene barbituric acids were found to be 5 orders of magnitude more electrophilic than quinone methides of comparable LUMO energies, indicating that the product stabilizing factor must be more important in the transition states of the former species. The conclusion drawn from Figure 10 that product stabilizing factors are less important in the reactions of DDQ with π-nucleophiles implies that SET processes can be expected to be more likely in reactions of DDQ with nucleophiles than in the corresponding reactions of benzhydrylium ions having similar electrophilicity E.

The kinetics of one-electron oxidations of silylated enol ethers and ketene acetals as well as of allylsilanes with one electron oxidants have previously been studied by Fukuzumi and co-workers.[15] The oxidation potentials of these π-systems as well as the intrinsic barriers for the electron transfer oxidation of these compounds by one-electron oxidants were derived from experimental rate constants using the Rehm–Weller Gibbs relationship (4), which derives the Gibbs energy of activation for the electron transfer ($\Delta G^{\ddagger}_{et}$) from the Gibbs energy of electron transfer (ΔG^{0}_{et} given by eq 5) and the intrinsic barrier ($\Delta G^{\ddagger}_{0,et}$). The latter quantity represents the Gibbs activation free energy for a process where the driving force of electron transfer is zero, i.e. $\Delta G^{\ddagger}_{et} = \Delta G^{\ddagger}_{0,et}$ for $\Delta G^{0}_{et} = 0$. Due to the significant rearrangements of structure accompanying electron transfer, large intrinsic barriers $\Delta G^{\ddagger}_{0,et}$ (15–20 kJ mol^{-1}) were observed for the one-electron oxidation of a large variety of silylated π-nucleophiles, including several compounds shown in Figure 8.

By applying the same methodology, we have now used the oxidation potentials in Table 3 to calculate the rate constants for the outer-sphere electron transfer of the reactions of DDQ

dx.doi.org/10.1021/ja405890d | J. Am. Chem. Soc. 2013, 135, 12377–12387

with the π-nucleophiles **2a**–**n** according to eqs 3–5, assuming an intrinsic barrier of $\Delta G^{\ddagger}_{0,et}$ = 18 kJ mol^{-1}, a typical value for such systems according to ref 15.

$$k_{et} = (k_b T/h)\exp(-\Delta G^{\ddagger}_{et}/RT) \quad (3)$$

$$\Delta G^{\ddagger}_{et} = \Delta G^{0}_{et}/2 + [(\Delta G^{0}_{et}/2)^2 + (\Delta G^{\ddagger}_{0,et})^2]^{1/2} \quad (4)$$

$$\Delta G^{0}_{et} = F(E_{ox} - E_{red}) \quad (5)$$

A plot of experimental rate constants log k_C (●) and log k_O (○) for the reactions of DDQ with various π-nucleophiles versus the calculated rates for SET (log k_{et}, from eqs 3–5) is presented in Figure 11. The open circles for systems which

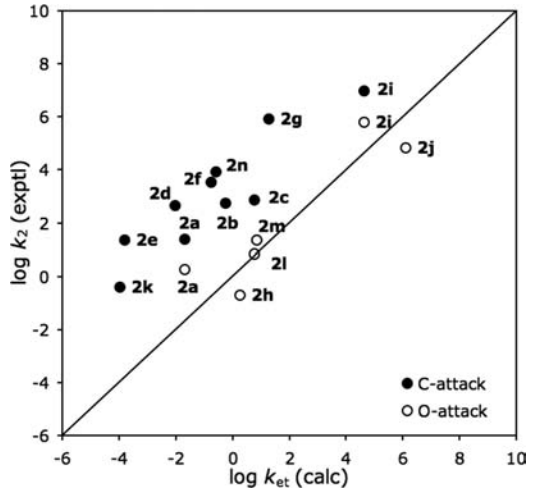

Figure 11. Correlation of experimental rate constants (log k_2, in CH_3CN) with calculated rate constants for SET (log k_{et}).

react via O attack are close to the diagonal, indicating that these reactions proceed with rates as expected for SET processes, while C attack at DDQ (filled circles) is 2 to 5 orders of magnitude faster than calculated for SET processes. We, therefore, conclude that C attack at DDQ usually occurs by a polar mechanism, which may be reversible if there is no fast subsequent reaction.

It should be noted that all experimental rate constants for the reactions of benzhydrylium ions with π-nucleophiles have been reported to be at least 8 orders of magnitude larger than the calculated rate constants for one-electron transfer processes.[17] Therefore, the reactions of DDQ with π-nucleophiles are generally closer to the borderline between polar reactions and electron transfer than the corresponding reactions of benzhydrylium ions (with π-nucleophiles).

Outer Sphere Electron Transfer (OSET) vs Inner Sphere Electron Transfer (ISET): Radical Clock Experiments. According to Figure 11, the observed rate constant for the reaction of **2j** with DDQ corresponds to that expected for a SET process. In order to examine the occurrence of an OSET mechanism, a radical clock[19] substrate **13** was designed based on the structure of **2j** (Scheme 14). When **13** was combined with DDQ, only **14**, the product of O attack, was observed in the ^{1}H NMR spectrum of the crude material (>95%), and **15** was isolated in 60% yield after column chromatography, while no cyclization product was observed (Scheme 15). Though cyclization of the radical cation **16** may be slower than analogous cyclizations of radicals, the quantitative formation of

Scheme 14. Synthesis of the Radical Clock Substrate 13

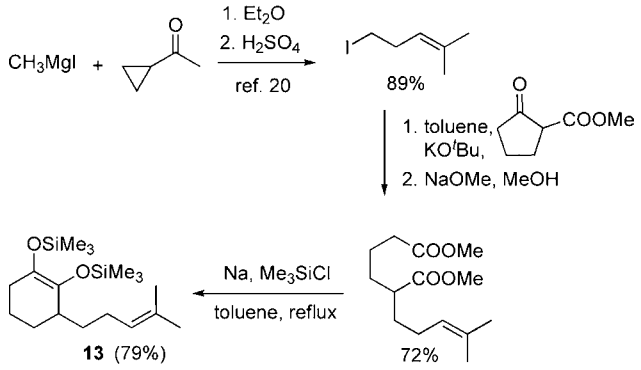

Scheme 15. Exclusion of OSET by a Radical Clock Experiment (CH_3CN, 20 °C)

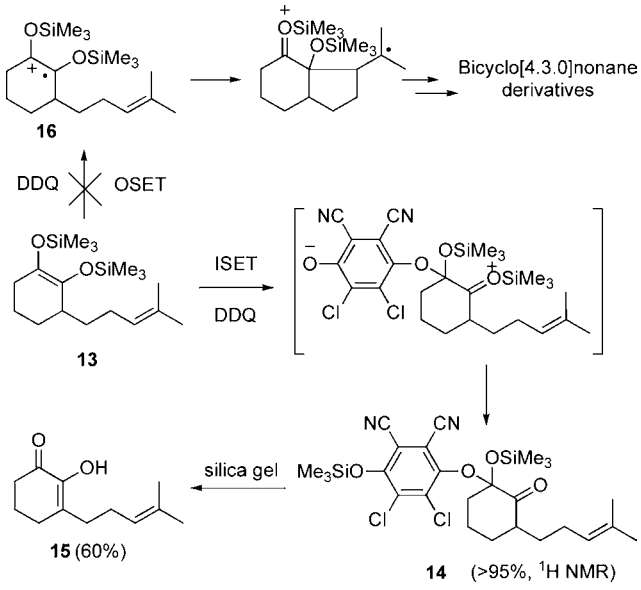

14 allows us to exclude the operation of an OSET mechanism because Mattay's report on the formation of carbocycles via photoinduced electron transfer oxidative cyclization of silyl enol ethers carrying side chains with olefinic double bonds indicates cyclizations of the intermediate radical cations to be faster than competing intermolecular processes.[21] Therefore, O attack is suggested to proceed via an ISET mechanism.

■ CONCLUSION

π-nucleophiles attack DDQ either at C-2 to give 4-hydroxycyclohexadienones or at oxygen to give O-substituted hydroquinones. In several cases initial C attack and subsequent rearrangement to the thermodynamically more stable products of O attack has been observed. Kinetics for the reactions of π-systems with DDQ have been determined photometrically, and it was found that the rate constants k_C for the attack of the π-nucleophiles **2** at C-2 of DDQ can be described by the linear free energy relationship (1), which allowed us to derive the electrophilicity parameter E = −3.66 for the C-2 position of DDQ. It thus possesses an electrophilic reactivity comparable to the flavylium and tropylium ion, and is considerably more reactive than the bis(dimethylamino)-substituted benzhydrylium ion or other highly reactive Michael acceptors (Figure 12).[8,9a]

dx.doi.org/10.1021/ja405890d | J. Am. Chem. Soc. 2013, 135, 12377–12387

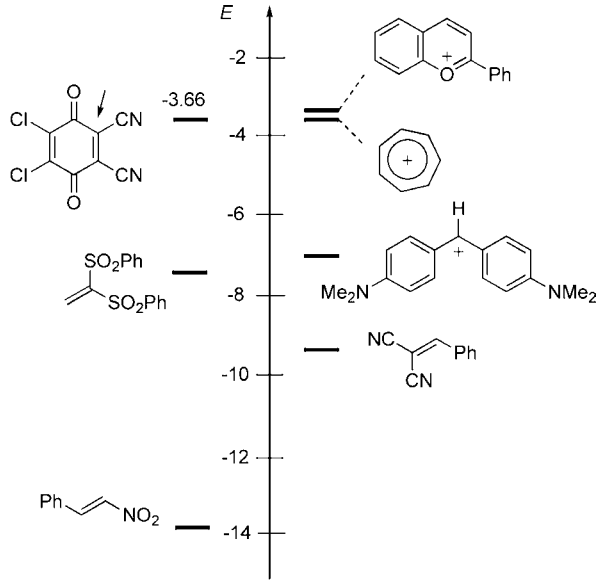

Figure 12. Comparison of the electrophilic reactivity of DDQ with that of other electrophiles.[8]

The experimental rate constants for the attack of π-systems at C-2 of DDQ are larger than those calculated for SET processes from the electrochemical oxidation potentials of the π-systems and the reduction potential of DDQ, indicating that C attack at DDQ usually occurs via polar processes. However, DDQ reacts about 12 orders of magnitude more slowly than benzhydrylium ions of comparable reduction potential showing that the transition states of the reactions of DDQ with π_{CC} systems profit much less from the formation of the new CC-bond (product stabilizing factor) than the corresponding reactions of benzhydrylium ions, which can be explained by the high stabilization of the DDQ radical anion. O-Attack is probably restricted to reactions with sterically shielded nucleophiles or to cases, where the faster C attack is highly reversible because the resulting intermediate cannot undergo fast subsequent reactions. The observed rate constants for O attack are smaller than calculated by eq 1 and thus are similar to those for SET processes (Scheme 16).

Since the radical-clock experiment did not provide evidence for the intermediacy of radical cations of the silylated enol ethers, these reactions are interpreted as inner sphere electron transfer processes.

Scheme 16. C versus O Attack in Reactions of DDQ with π-Nucleophiles

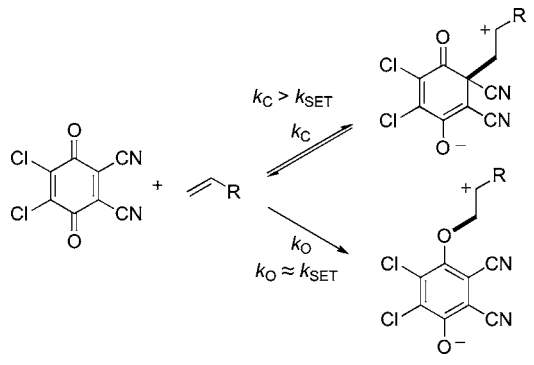

EXPERIMENTAL SECTION

Materials. DDQ was purchased from ABCR and recrystallized from chloroform or dichloromethane before use. Silyl enol ethers **2(a-e, a′, h)** were prepared as reported in the literature.[22] Silyl ketene acetals **2(f, g, i)** were prepared according to ref 23. The synthesis of disiloxy hexane **2j** was achieved by Rühlmann-type acyloin condensation.[24] Enamino esters **2l** and **2m** were prepared from amines and methyl propiolate. Diazomethanes **2n** and **2o** were prepared according to refs 25 and 26, respectively.

Kinetics. All of the rates of reactions were determined photometrically in dry acetonitrile or in freshly distilled dry CH_2Cl_2. Fast reactions were determined by using the stopped-flow technique. Slow reactions were measured by conventional photodiode array UV−vis spectrometers. The temperature was kept constant at 20 ± 0.1 °C by using a circulating bath thermostat. In all runs, excess of nucleophiles (at least 8-fold) over DDQ was used to achieve pseudo first-order kinetics.

ASSOCIATED CONTENT

Supporting Information

Details of the kinetic experiments, synthetic procedures, X-ray crystal structure determination, and quantum chemical calculations as well as NMR spectra of all characterized compounds. This material is available free of charge via the Internet at http://pubs.acs.org.

AUTHOR INFORMATION

Corresponding Author

herbert.mayr@cup.uni-muenchen.de

Notes

The authors declare no competing financial interest.

ACKNOWLEDGMENTS

Dedicated to Professor Helmut Schwarz on the occasion of his 70th birthday. We thank the Deutsche Forschungsgemeinschaft (SFB 749, Project B1) and the China Scholarship Council (fellowship to X.G.) for financial support. We are grateful to Dr. Peter Mayer for the X-ray diffraction experiments. Furthermore, we thank Dr. Armin R. Ofial for help during preparation of this manuscript.

REFERENCES

(1) Thiele, J.; Günther, F. *Liebigs Ann. Chem.* **1906**, *349*, 45−66.
(2) Andrieux, C. P.; Merz, A.; Saveant, J.-M.; Tomahogh, R. *J. Am. Chem. Soc.* **1984**, *106*, 1957−1962.
(3) (a) Walker, D.; Hiebert, J. D. *Chem. Rev.* **1967**, *67*, 153−195. (b) Becker, H.-D. In *The Chemistry of the Quinoid Compounds, Part I*; Patai, S., Ed.; Wiley: Chichester, U.K., 1974; pp 335−423. (c) Becker, H.-D.; Turner, A. B. In *The Chemistry of the Quinoid Compounds Vol. 2*; Patai, S., Rappoport, Z., Eds.; Wiley: Chichester, U.K., 1988; pp 1351−1384. (d) Buckle, D. R. In *Encyclopedia of Reagents for Organic Synthesis Vol. 3*; Paquette, L. A., Ed.; Wiley: Chichester, U.K., 1995; p 1699.
(4) (a) Zhang, Y.; Li, C.-J. *Angew. Chem., Int. Ed.* **2006**, *45*, 1949−1952. (b) Zhang, Y.; Li, C.-J. *J. Am. Chem. Soc.* **2006**, *128*, 4242−4243. (c) Tu, W.; Floreancig, P. E. *Angew. Chem., Int. Ed.* **2009**, *48*, 4567−4571. (d) Liu, L.; Floreancig, P. E. *Angew. Chem., Int. Ed.* **2010**, *49*, 3069−3072. (e) Guo, C.; Song, J.; Luo, S.-W.; Gong, L.-Z. *Angew. Chem., Int. Ed.* **2010**, *49*, 5558−5562. (f) Liu, L.; Floreancig, P. E. *Angew. Chem., Int. Ed.* **2010**, *49*, 5894−5897. (g) Hayashi, Y.; Itoh, T.; Ishikawa, H. *Angew. Chem., Int. Ed.* **2011**, *50*, 3920−3924. (h) Tsang, A. S.-K.; Jensen, P.; Hook, J. M.; Hashmi, A. S. K.; Todd, M. H. *Pure Appl. Chem.* **2011**, *83*, 655−665. (i) Alagiri, K.; Devadig, P.; Prabhu, K. R. *Chem.—Eur. J.* **2012**, *18*, 5160−5164. (j) Rohlmann, R.; Garcia Mancheño, O. *Synlett* **2013**, *24*, 6−10.
(5) Bhattacharya, A.; DiMichele, L. M.; Dolling, U.-H.; Douglas, A. W.; Grabowski, E. J. J. *J. Am. Chem. Soc.* **1988**, *110*, 3318−3319.

(6) (a) Bhattacharya, A.; DiMichele, L. M.; Dolling, U.-H.; Grabowski, E. J. J.; Grenda, V. J. *J. Org. Chem.* **1989**, *54*, 6118−6120. (b) For an earlier report on the formation of enones by oxidation of silyl enol ethers with DDQ, see: Ryu, I.; Murai, S.; Hatayama, Y.; Sonoda, N. *Tetrahedron Lett.* **1978**, *19*, 3455−3458.
(7) (a) Mayr, H.; Patz, M. *Angew. Chem., Int. Ed. Engl.* **1994**, *33*, 938−957. (b) Mayr, H.; Ofial, A. R. *Pure Appl. Chem.* **2005**, *77*, 1807−1821. (c) Mayr, H.; Ofial, A. R. *J. Phys. Org. Chem.* **2008**, *21*, 584−595. (d) Mayr, H.; Kempf, B.; Ofial, A. R. *Acc. Chem. Res.* **2003**, *36*, 66−77.
(8) For a comprehensive database of nucleophilicity parameters *N* and s_N as well as electrophilicity parameters *E*, see: http://www.cup.lmu.de/oc/mayr/DBintro.html.
(9) (a) Mayr, H.; Bug, T.; Gotta, M. F.; Hering, N.; Irrgang, B.; Janker, B.; Kempf, B.; Loos, R.; Ofial, A. R.; Remennikov, G.; Schimmel, H. *J. Am. Chem. Soc.* **2001**, *123*, 9500−9512. (b) Lucius, R.; Loos, R.; Mayr, H. *Angew. Chem., Int. Ed.* **2002**, *41*, 91−95. (c) Richter, D.; Hampel, N.; Singer, T.; Ofial, A. R.; Mayr, H. *Eur. J. Org. Chem.* **2009**, 3203−3211. (d) Ammer, J.; Nolte, C.; Mayr, H. *J. Am. Chem. Soc.* **2012**, *134*, 13902−13911.
(10) Kucklaender, U.; Bollig, R.; Frank, W.; Gratz, A.; Jose, J. *Bioorg. Med. Chem.* **2011**, *19*, 2666−2674.
(11) (a) Mulliken, R. S.; Person, W. B. *Molecular Complexes*; Wiley-Interscience: New York, 1969. (b) Mataga, N.; Kubota, T. *Molecular Interactions and Electronic Spectra*; Marcel Dekker: New York, 1970.
(12) (a) Seeman, J. I. *Chem. Rev.* **1983**, *83*, 83−134. (b) Curtin, D. Y. *Rec. Chem. Prog.* **1954**, *15*, 111. (c) Hammett, L. P. *Physical Organic Chemistry*; McGraw-Hill: New York, 1970.
(13) Frisch, M. J.; Trucks, G. W.; Schlegel, H.; Scuseria, G. E.; Robb, M. A.; Cheeseman, J. R.; Scalmani, G.; Barone, V.; Mennucci, B.; Petersson, G. A.; Nakatsuji, H.; Caricato, M.; Li, X.; Hratchian, H. P.; Izmaylov, A. F.; Bloino, J.; Zheng, G.; Sonnenberg, J. L.; Hada, M.; Ehara, M.; Toyota, K.; Fukuda, R.; Hasegawa, J.; Ishida, M.; Nakajima, T.; Honda, Y.; Kitao, O.; Nakai, H.; Vreven, T.; Montgomery, J. A.; Peralta, J. E.; Ogliaro, F.; Bearpark, M.; Heyd, J. J.; Brothers, E.; Kudin, K. N.; Staroverov, V. N.; Kobayashi, R.; Normand, J.; Raghavachari, K.; Rendell, A.; Burant, J. C.; Iyengar, S. S.; Tomasi, J.; Cossi, M.; Rega, N.; Millam, J. M.; Klene, M.; Knox, J. E.; Cross, J. B.; Bakken, V.; Adamo, C.; Jaramillo, J.; Gomperts, R.; Stratmann, R. E.; Yazyev, O.; Austin, A. J.; Cammi, R.; Pomelli, C.; Ochterski, J. W.; Martin, R. L.; Morokuma, K.; Zakrzewski, V. G.; Voth, G. A.; Salvador, P.; Dannenberg, J. J.; Dapprich, S.; Daniels, A. D.; Farkas; Foresman, J. B.; Ortiz, J. V.; Cioslowski, J.; Fox, D. J. *Gaussian 09*, revision A.02; Gaussian, Inc.: Wallingford, CT, 2009.
(14) Henry, D. J.; Sullivan, M. B.; Radom, L. *J. Chem. Phys.* **2003**, *118*, 4849−4860.
(15) Fukuzumi, S.; Fujita, M.; Otera, J.; Fujita, Y. *J. Am. Chem. Soc.* **1992**, *114*, 10271−10278.
(16) Pysh, E. S.; Yang, N. C. *J. Am. Chem. Soc.* **1963**, *85*, 2124−2130.
(17) Ofial, A. R.; Ohkubo, K.; Fukuzumi, S.; Lucius, R.; Mayr, H. *J. Am. Chem. Soc.* **2003**, *125*, 10906−10912.
(18) Zhou, L.-G.; Liao, W.; Yu, Z.-X. *Asian J. Org. Chem.* **2012**, *1*, 336−345.
(19) (a) Newcomb, M.; Curran, D. P. *Acc. Chem. Res.* **1988**, *21*, 206−214. (b) Tolbert, L. M.; Sun, X.-J.; Ashby, E. C. *J. Am. Chem. Soc.* **1995**, *117*, 2681−2685. (c) Zard, S. Z. *Radical Reactions in Organic Synthesis*; Oxford University Press: New York, 2003.
(20) Liu, Z.; Peng, L.; Zhang, T.; Li, Y. L. *Synth. Commun.* **2001**, *31*, 2549−2555.
(21) (a) Bunte, J. O.; Rinne, S.; Schäfer, C.; Neumann, B.; Stammler, H.-G.; Mattay, J. *Tetrahedron Lett.* **2003**, *44*, 45−48. (b) MacMillan's observation of the intramolecular attack of an enamine radical cation at a 1,2-dialkylated ethylene with formation of a five-membered ring, which has a much lower driving-force confirms this conclusion: Beeson, T. D.; Mastracchio, A.; Hong, J.-B.; Ashton, K.; MacMillan, D. W. C. *Science* **2007**, *316*, 582−585.
(22) (a) Cazeau, P.; Duboudin, F.; Moulines, F.; Babot, O.; Dunogues, J. *Tetrahedron* **1987**, *43*, 2075−2088. (b) Cazeau, P.; Duboudin, F.; Moulines, F.; Babot, O.; Dunogues, J. *Tetrahedron* **1987**, *43*, 2089−2100.
(23) Oisaki, K.; Suto, Y.; Kanai, M.; Shibasaki, M. *J. Am. Chem. Soc.* **2003**, *125*, 5644−5645.
(24) Rühlmann, K. *Synthesis* **1971**, 236−253.
(25) Wulfman, D. S.; Yousefian, S.; White, J. M. *Synth. Commun.* **1988**, *18*, 2349−2352.
(26) Searle, N. E. *Org. Synth.* **1956**, *36*, 25−27.